CIB-W18/43-21-2

A NEW METHOD TO DETERMINE SUITABLE SPACINGS AND DISTANCES FOR SELF-TAPPING SCREWS

T Uibel

H J Blaß

Timber Structures and Building Construction

Karlsruhe Institute of Technology (KIT)

GERMANY

A New Method to Determine Suitable Spacings and Distances for Self-tapping Screws

T. Uibel, H.J. Blaß
Timber Structures and Building Construction
Karlsruhe Institute of Technology (KIT), Germany

1 Introduction

In recent years self-tapping screws have been increasingly used for connections or reinforcements in timber engineering. Most self-tapping screws can be arranged maintaining only small spacings and distances without risking a consequential splitting failure of the timber member. To avoid significant crack growth and splitting failure minimum values for spacings, end and edge distances as well as for the corresponding minimum timber thickness have to be determined. These requirements are important for the design of joints with self-tapping screws and have to be defined in technical approvals or to be examined regarding structural design codes [1] [2]. Fig. 1 shows typical splitting failure due to too small spacings and distances. The determination of spacing, edge and end distance requirements for self-tapping screws requires numerous and comprehensive insertion tests. Yet the results of such tests cannot be transferred to other types of screws or even to screws of different diameter because of differences in shape or geometry. To reduce the effort of insertion tests a new method was developed which allows the estimation of required spacings, distances and timber thickness.

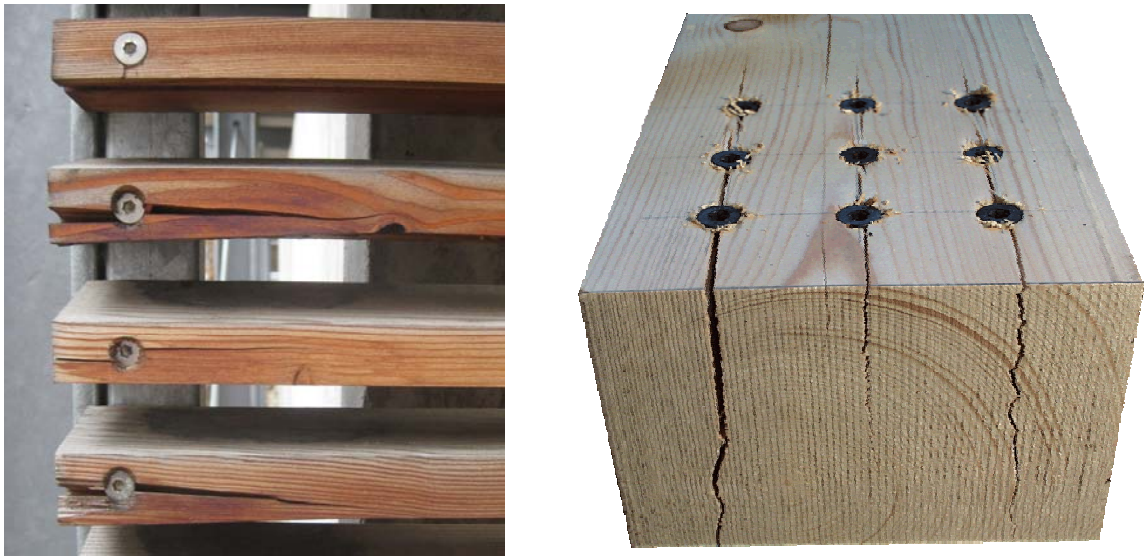

Fig. 1: Typical splitting failure caused by the insertion of self-tapping screws

2 Conventional insertion tests

Concerning spacing and distance requirements self-tapping screws are usually treated like nails without pre-drilled holes. Often, self-tapping screws may be arranged with smaller spacings, end and edge distances than currently specified in the German design code DIN 1052 [1] or in EN 1995-1-1 [2] without risking a splitting failure. Fig. 2 shows the minimum values which are provided by the German design code DIN 1052 [1]. For many types of self-tapping screws reduced spacings and distances are possible as e.g. for nails with predrilled holes. This particularly depends on the shape of the screw tip and head and on the existence of special features decreasing the torsional resistance to insertion. Fig. 3 shows the great variety of screw tips and heads.

As yet insertion tests (here called "conventional insertion tests") are carried out in order to determine suitable spacings and distances. For a conventional insertion test the examined self-tapping screw is inserted without pre-drilling as usual in practice. The screw head should be flush with the timber surface. The test specimens have to be made of sawn timber of higher density. After the insertion the crack growth has to be evaluated. To identify possible combinations of spacings, end distances and cross-sections it is necessary to test different configurations iteratively. Table 1 shows the results of 326 conventional insertion tests with five types of self-tapping screws of four manufacturers [3]. The tests were carried out with different configurations so that altogether 1125 screws were used. It was the aim of the tests to determine the minimum timber thickness necessary to avoid undue splitting by arranging the self-tapping screws with the same spacings, end and edge distances as for nails with predrilled holes (last column of the table given in Fig. 2).

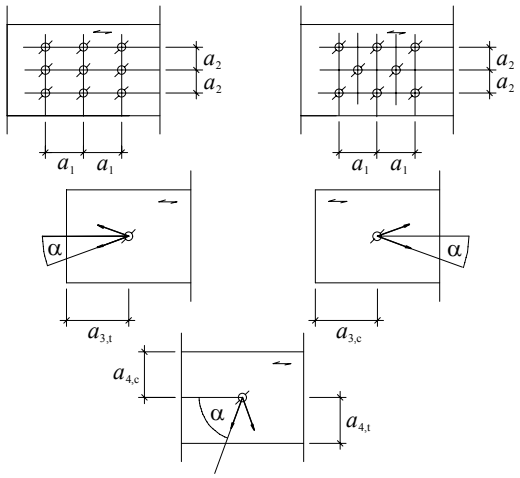

Spacing or distance	without predrilled holes[1)]		with predrilled holes
	$d < 5$ mm	$d \geq 5$ mm	
a_1	$(5+5 \cos \alpha)\, d$	$(5+7 \cos \alpha)\, d$	$(3+2 \cos \alpha)\, d$
a_2	$5\, d$	$5\, d$	$3\, d$
$a_{3,t}$	$(7+5 \cos \alpha)\, d$	$(10+5 \cos \alpha)\, d$	$(7+5 \cos \alpha)\, d$
$a_{3,c}$	$7\, d$	$10\, d$	$7\, d$
$a_{4,t}$	$(5+2 \sin \alpha)\, d$	$(5+5 \sin \alpha)\, d$	$(3+4 \sin \alpha)\, d$
$a_{4,c}$	$5\, d$	$5\, d$	$3\, d$
1) for timber of a characteristic density $\rho_k \leq 420$ kg/m³			

Fig. 2: Minimum spacings, end and edge distances according to German DIN 1052 [1]

Fig. 3: Different tips and heads of self-tapping screws

The mean density (at normal climate, 20°C/65% RH) of all specimens made of European spruce (*Picea abies*) or fir (*Abies alba*) was $\rho_m = 484$ kg/m³ and the mean moisture content $u_m = 12{,}0$ %. The determined minimum timber thickness for each screw type and diameter is given in Table 1. The test results show that the intended spacings and distances are possible for all types of examined self-tapping screws. For some types of screws minor restrictions concerning the end distance $a_{3,c}$ and the spacing a_1 need to be set. The determined corresponding minimum timber thickness is very different depending on the screw type and diameter. The reasons for these discrepancies are differences in screws' geometry or in special features decreasing the torsional resistance e.g. the shape of the screw tips and their effects of pre-drilling. In consequence the results of conventional insertion tests cannot be transferred to other types of screws or even to screws of different diameter. Furthermore the evaluation of insertion tests is ambiguous because it is only based on externally visible cracks. For these reasons the extent of insertion tests and the effort involved in these tests is large.

Table 1: Results of conventional insertion tests with five types of self-tapping screws

Producer / Type	d mm	ρ_{mean} kg/m³	n_{test}	t_{min} mm		End distance and spacing restrictions
A	5	487	51	24	$4{,}8 \cdot d$	$a_{3,c} \geq 12 \cdot d$; $a_1 \geq 5 \cdot d$
A-2	5	483	56	30	$6 \cdot d$	$a_{3,c} \geq 12 \cdot d$; $a_1 \geq 5 \cdot d$
A	8	477	35	80	$10 \cdot d$	-
A	10	497	12	100	$10 \cdot d$	$a_{3,c} \geq 12 \cdot d$; $a_1 \geq 5 \cdot d$
A	12	449	42	96	$8 \cdot d$	$a_{3,c} \geq 12 \cdot d$; $a_1 \geq 5 \cdot d$
B	8	497	13	40	$5 \cdot d$	$a_{3,c} \geq 12 \cdot d$; $a_1 \geq 5 \cdot d$
C	6	504	51	42	$7 \cdot d$	-
C	8	484	44	64	$8 \cdot d$	-
D	8,9	494	22	127	$14{,}3 \cdot d$	$a_{3,c} \geq 12 \cdot d$; $a_1 \geq 5 \cdot d$

3 Test method for determining screw-specific influences

In order to reduce the effort involved in determining suitable spacings, end and edge distances as well as the corresponding timber thickness for self-tapping screws it was the objective of a research project [4] to develop a calculation method which allows an estimation of the splitting behaviour of timber during the insertion process. Therefore the influences which are important for the splitting behaviour have to be taken into account. They may be classified into three groups: Material-specific influences (e.g. wood species, density, width of growth rings and their orientation, moisture content), geometry-specific influences (spacings, end and edge distances in relation to the screw diameter, position and number of screws), fastener-specific influences (e.g. shape of the screw tip, screw head, further features to decrease the torsional resistance). By using a numerical calculation model on the basis of the Finite Element Method almost all of the material-specific and geometry-specific influences on the splitting behaviour can be covered. But so far it is not possible to model the insertion process directly using the Finite Element Method, particularly with regard to the screw-specific influences.

In order to determine the fastener-specific influences on the splitting behaviour a new test method was developed for measuring forces affecting the member perpendicular to the grain during the insertion process [4]. Fig. 4 shows the test set-up. For the test a two-part specimen of solid wood, glued laminated timber or laminated veneer lumber is required.

The two-part specimen is made of one cross-section by sawing it parallel to the grain, as shown in Fig. 5. The two parts of the test specimen are connected with bolts which are used as measuring elements. These measurement bolts are tightened with a defined force. A strain gauge is bonded into a hole drilled at the centre of the measurement bolt. By calibrating the strain gauge bonded in the measurement bolt it is possible to measure axial forces. The examined screw is driven into the interface of the two parts of the test specimen. For the insertion process a screw-testing machine (Fig. 4) is used, so that the rotation speed is constant. Furthermore it is possible to measure the screw insertion moment and to control the penetration depth. The screw is inserted using a template to avoid an inclination of the screw. After the insertion the indentation depth of the root of the screw thread should be similar on both parts of the test specimen, as shown in the example of an opened test specimen in Fig. 5.

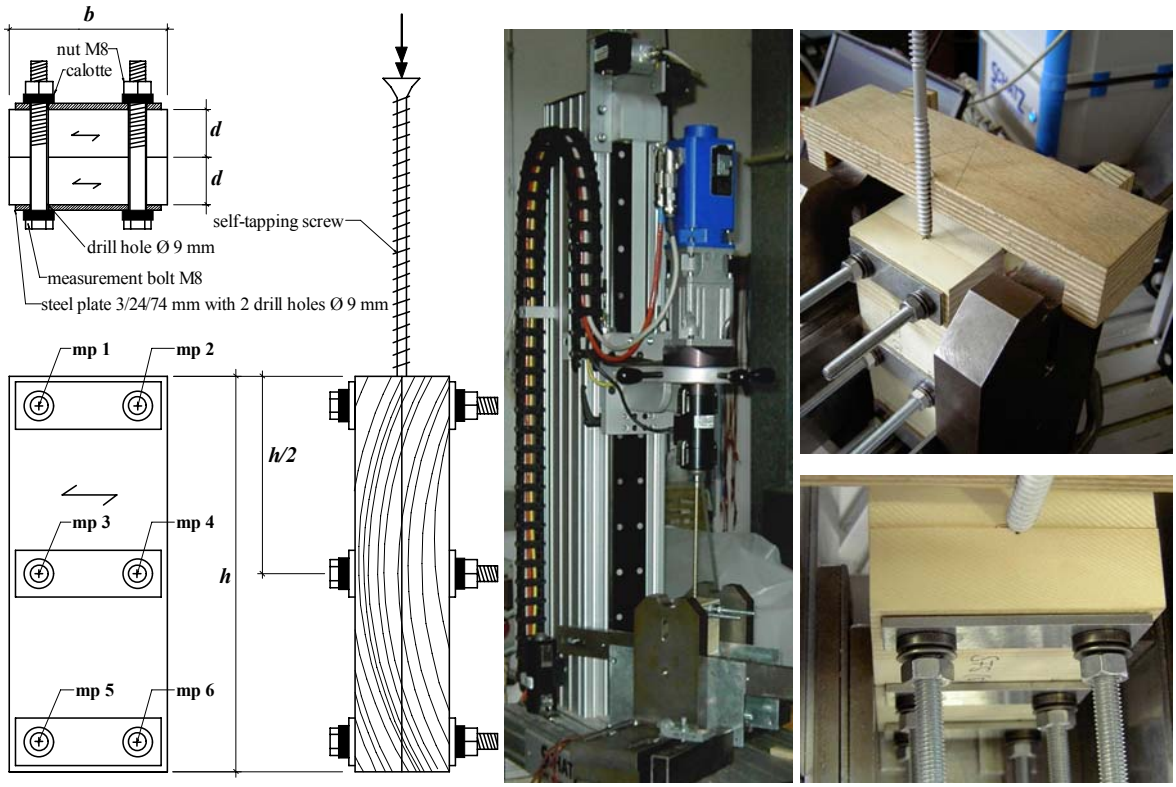

Fig. 4: Test set-up with position of measurement points (mp) 1 to 6

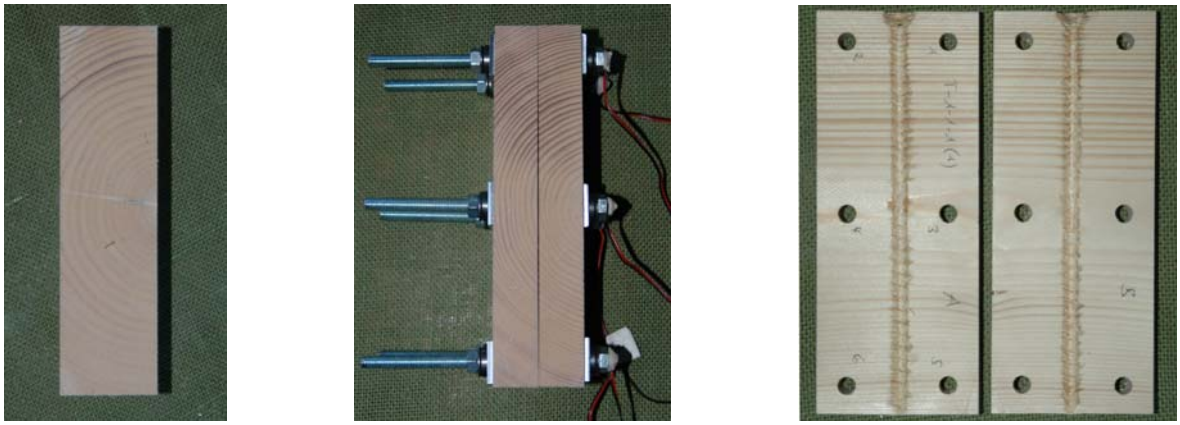

Fig. 5: Two-part test specimen connected with measurement bolts (middle) made of one cross section (left), opened specimen after the test (right)

The test method allows displaying the forces acting on the test specimen, measured at the measuring points, over the penetration depth during the insertion process. The positions of the measurement bolts (measuring points) 1 to 6 are marked in Fig. 4. To compare the splitting behaviour of screws from three manufactures (A, B, C) three test series with altogether 97 tests were carried out. In each series screws of the three different types (A, B, C) with 8.0 x 200 mm in dimension were tested. The parameter of the specimens and the test results are presented in Table 2. It was possible to determine significant force-penetration depth curves for the different types of screw. Fig. 6 shows the results of one test series (series 1). In order to compare the test results directly specimens with the same material properties were used in the different sub-series (e.g. 1-A, 1-B, 1-C). This was realised by using one scantling for the production of several specimens, which were allocated to the different sub-series.

For further comparisons the mean total force $F_{m,tot}$ is defined. This is the sum of all measured forces ($F_{mp,i}$) exerted on the six measurement bolts (i = 1 to 6) over the penetration depth (ℓ_{pd}), divided by the nominal screw length ($\ell_{sr,nom}$):

$$F_{m,tot} = \frac{1}{\ell_{sr,nom}} \int_0^{\ell_{pd}} \left(F_{mp,1}(x) + .. + F_{mp,i}(x) + .. + F_{mp,n}(x) \right) dx \quad \text{in N} \qquad (1)$$

with

$F_{m,tot}$ mean total force in N

$F_{mp,i}$ force at the measuring point i in N

ℓ_{pd} total penetration depth in mm

$\ell_{sr,nom}$ nominal screw length in mm

Instead of the nominal screw length $\ell_{sr,nom}$ the forces can be set in relation to the real screw length $\ell_{sr,real}$ or the total penetration length ℓ_{pd}.

To facilitate a comparison between the test results of the different series the mean total force for screw type A is used as a reference value, as shown in Table 2. The chosen comparison of indices also allows contrasting the results of the new test method with the minimum timber thickness determined by conventional insertion tests. A visualisation of this comparison is given in the bar chart in Fig. 7. It shows the good correspondence between the results of the two test methods. Thence the method allows a direct evaluation of a screw's effect on the splitting behaviour by comparing it with the results of parallel tests involving reference screws whose influence on the splitting behaviour has already been established.

Table 2: Results of tests with screw types A, B and C, 8.0 x 200 mm, series 1 to 3

Series	Screw type	Number of tests		Specimen dimensions $d/b/h$ mm	ρ_{mean} kg/m³	$E_{0,dyn,m}$ N/mm²	Mean total force			Minimum timber thickness	
		absolute	usable				$F_{m,tot}$ N	CoV %	Index %	t_{min} mm	Index %
1	A	10	9	24/80/180	453	12511	1646	9,67	100	$10 \cdot d$	100
	B	10	8		454	12659	886	10,0	54	$5 \cdot d$	50
	C	10	7		460	13102	1466	10,9	89	$8 \cdot d$	80
2	A	14	9	24/80/200	378	10249	1003	12,1	100	$10 \cdot d$	100
	B	10	10		391	11195	595	15,8	59	$5 \cdot d$	50
	C	10	10		387	11195	908	11,7	91	$8 \cdot d$	80
3	A	13	6	24/80/200	506	13691	1689	5,49	100	$10 \cdot d$	100
	B	10	7		507	13688	1013	8,06	60	$5 \cdot d$	50
	C	10	8		502	13898	1576	12,5	93	$8 \cdot d$	80
$E_{0,dyn,m}$ Mean value of the dynamic MOE from longitudinal vibration											

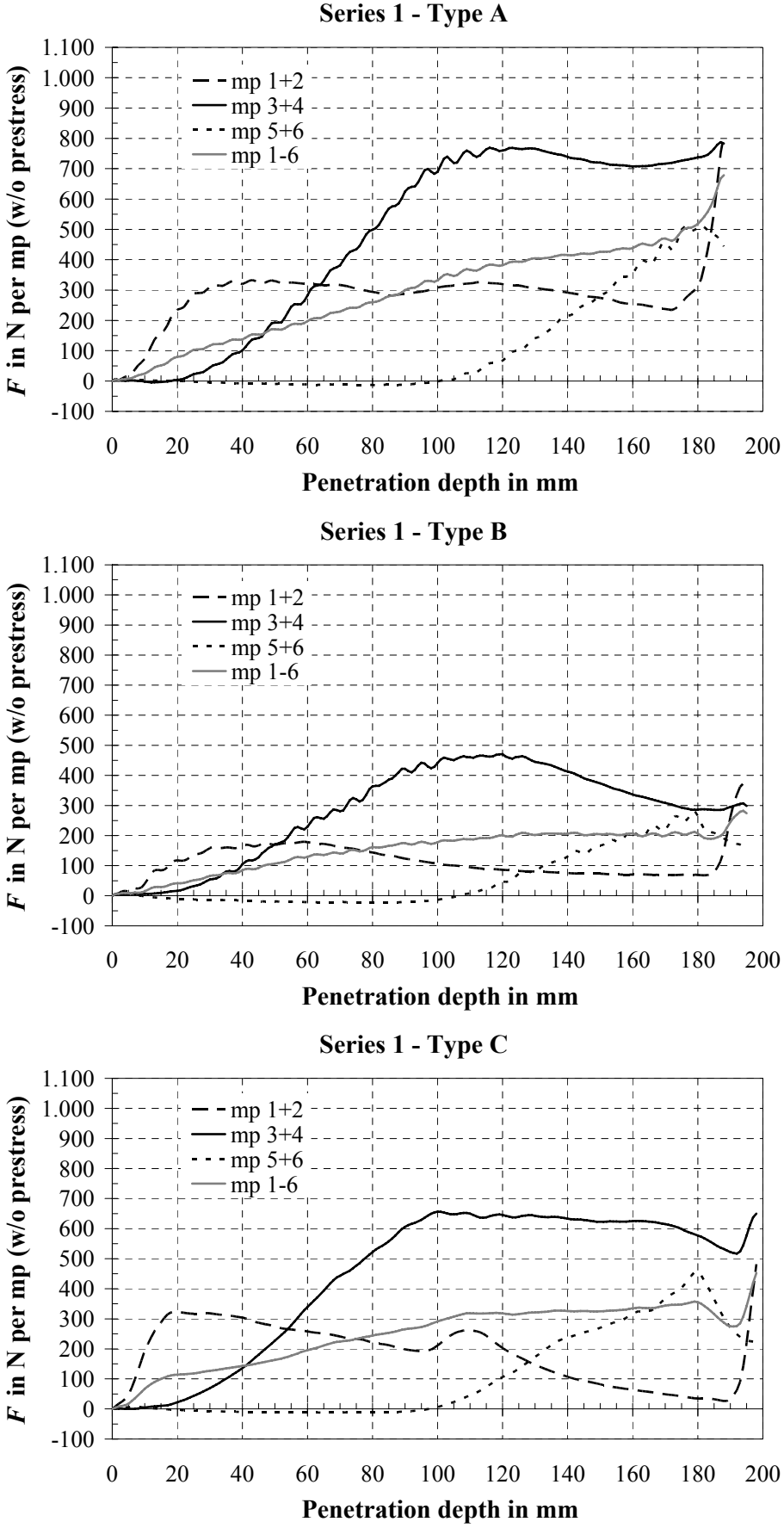

Fig. 6: Forces at the measurement points (mp) over penetration depth for screw types A, B and C, mean values of sub-series (1-A, 1-B, 1-C)

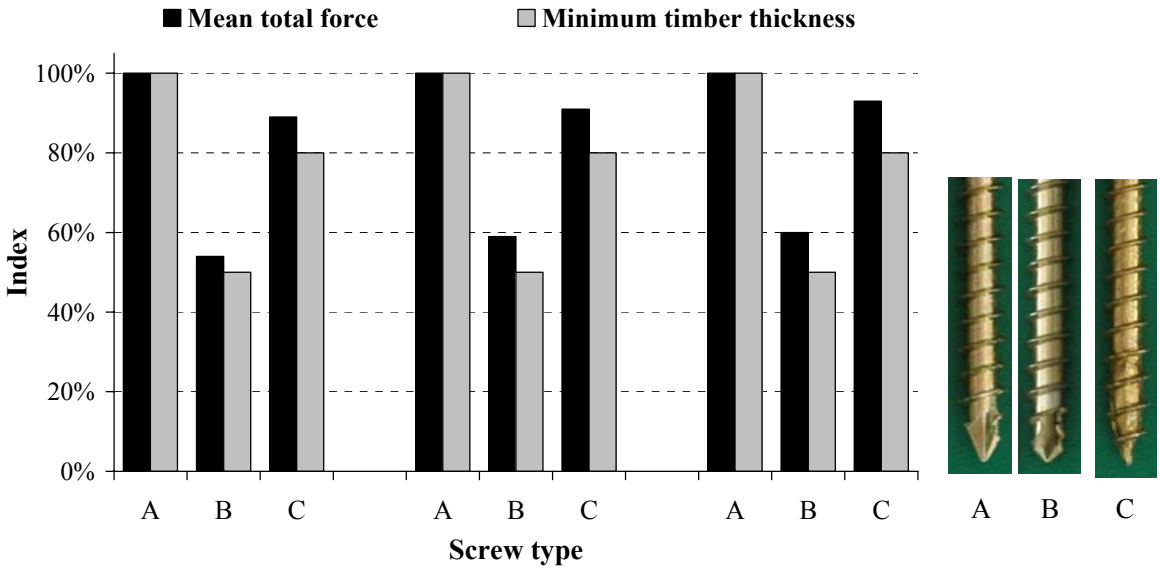

Fig. 7: Bar chart of indices of mean total force $F_{m,tot}$ and minimum timber thickness t_{min} for Series 1 to 3

The following parameters were examined systematically to analyse their influence on the forces acting on the timber during the insertion: geometry of the specimen (width b, height h, depth d as defined in Fig. 5), number of measurement bolts (6, 8, 10), screw length, ratio between screw length and specimen height, insertion speed, pre-stress of measurement bolts. Furthermore the following influences on the splitting forces or mean total forces were the focus of parameter studies: type and diameter of screws, density of the specimen, angle between screw axis and grain direction, angle γ between screw axis and growth ring tangent (Fig. 8) and moisture content of specimen.

The tests performed with specimens of sawn timber are not sufficient to determine the influences of the angle γ between the screw axis and the growth ring tangent. In the case of these specimens the angle γ varied between 0° and 90° depending on the position in specimen height. For an explicit analysis of the influence of γ special specimens of glued laminated timber produced in the laboratory from one lamella (Fig. 8) are used. For these specimens the angle γ is nearly constant over the full height.

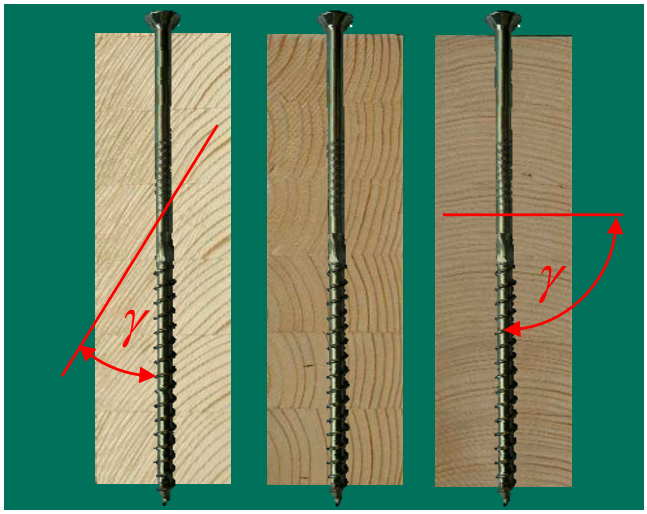

Fig. 8: Specimens to determine the influence of γ

4 Numerical and experimental analysis of split areas

4.1 Numerical model

Knowing the size of the resulting split area is important to evaluate the risk of splitting during the insertion process and hence to determine the required minimum timber thickness and minimum spacings, end and edge distances. Therefore a numerical model was developed to calculate the resulting crack area. For the numerical analysis the finite element program ANSYS 11.0 is used. Taking advantage of the symmetry conditions in the finite element model the timber member is modelled with volume elements. Fig. 9 shows a schematic sketch of the finite element model. In order to model the insertion process an equivalent moving load is used. The tensile strength perpendicular to the grain, which represents a relevant factor for splitting, is simulated by using non-linear spring-elements whose material behaviour was determined on the basis of tests using CT-specimens (Fig. 10) carried out by Schmid [6]. Therefore the tests with CT-specimens were calculated by using a two-dimensional FE model. Because of the symmetry only half the specimen was modelled and the spring elements were placed in the crack area. The parameters of the springs' force-deflection curve were varied until the best fit between test results and FE-calculation of the CT-specimens was reached. Fig. 10 shows a comparison of force-deflection curves of the test and of the FE-calculation for one CT-specimen (Fi02b). Altogether 47 CT-specimen made of *Picea abies* were used to calibrate the spring elements. The calculations resulted in the stress-deflection curve given in Fig. 11.

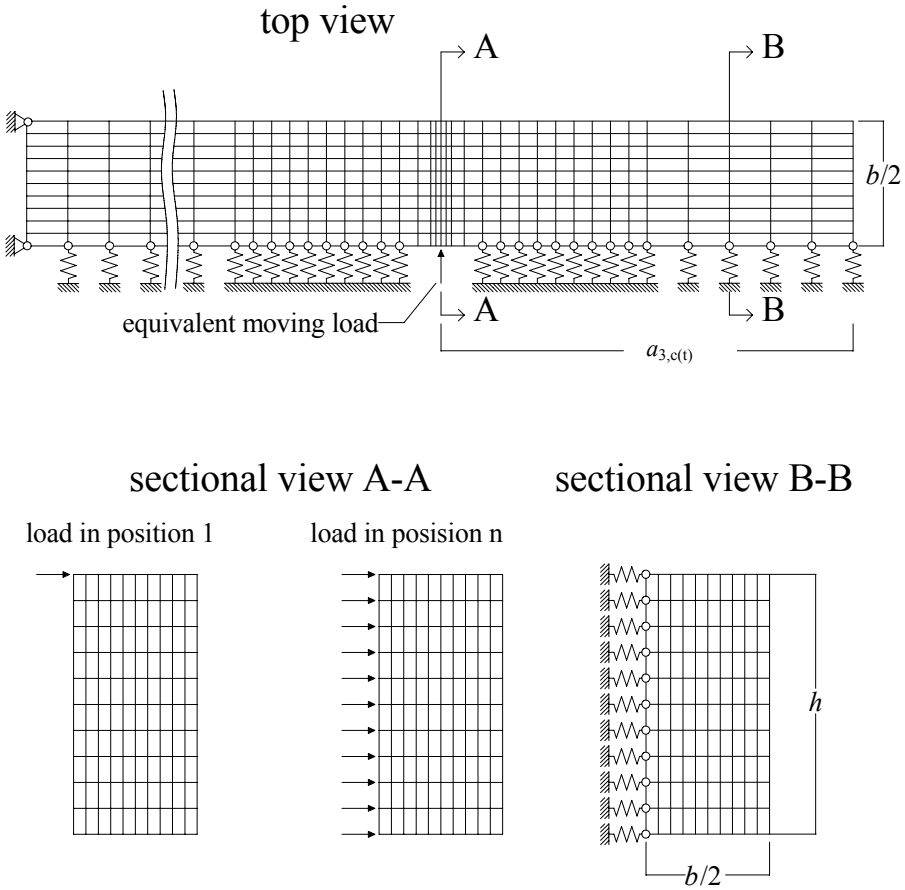

Fig. 9: Schematic sketch of the FE-model used to calculate split areas

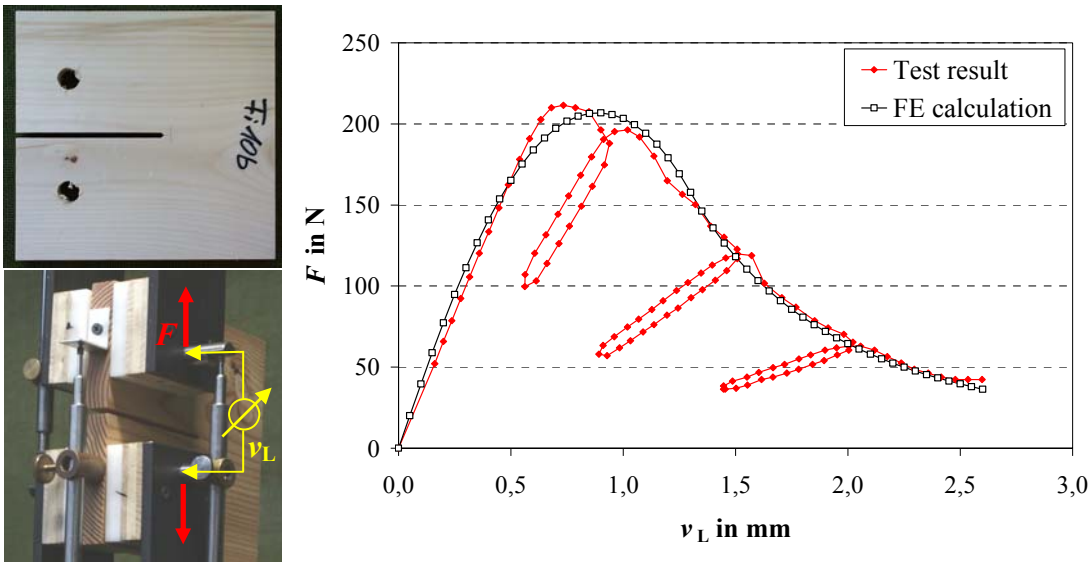

Fig. 10: CT-specimen and test set-up [6] (left), force-deflection curve of one test with a CT-specimen (Fi02b) and of the corresponding calculation

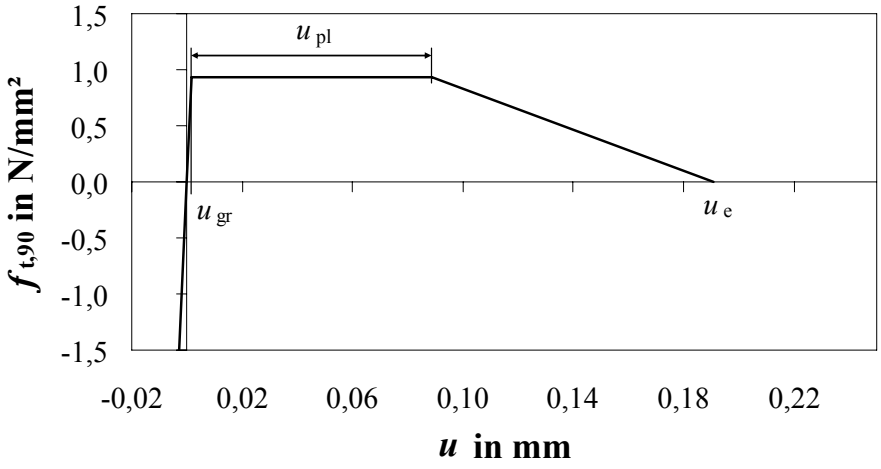

Fig. 11: Stress-deflection curve of the spring elements

4.2 Modelling the insertion process

So far it is not possible to model the insertion process directly using the Finite Element Method. To solve this modelling problem the forces exerted on the timber during the insertion process were meant to be determined on the basis of tests of the new method described in chapter 3. For this purpose the tests are simulated with a three dimensional finite element model. The insertion of the screw is modelled by an equivalent moving load (Fig. 8). This load has to be determined iteratively. Therefore the function of the load $q(x_{sr})$ is varied until the best fit between the force-penetration depth curves of calculations and test results is reached for each pair of measuring points. Fig. 8 (right) shows a comparison between calculated force-penetration depth curves and the test results for measuring points 1 to 6.

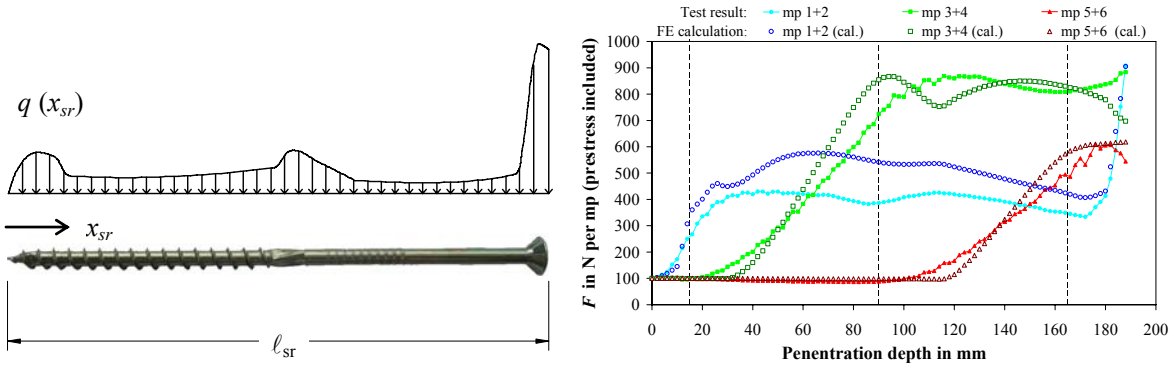

Fig. 12: Schematic representation of an equivalent moving load for screw type C to simulate the insertion process (left) and comparison of calculated force-penetration depth curves and test results for screw type A (right)

4.3 Determining the size of split areas by experimental studies

The calculation model which is used to determine the split areas has to be calibrated and to be verified. To that purpose the cracks were visualized in insertion tests by dyeing the relevant areas. Lau [5] used this method in a similar way for tests with nails. For these tests the screw is driven into and through the timber. The screw should be inserted using a template to avoid an unwanted inclination of the screw. Friction effects reducing the splitting tendency should be eliminated. After the insertion the screw is unscrewed. The screw has produced a hole in the timber. This hole is sealed where the screw tip exits the specimen at the timber surface, e.g. by using a tape. Subsequently a low-viscosity dye is filled into the hole. The dye is distributed by capillary action into the cracks and colours the split area. After the dye has dried, the coloured split areas are made visible by opening the specimens along the split surface. At the opened specimen the size of the split area caused by the insertion of the screw can be quantified e.g. using a digital measuring projector. Fig. 13 shows a typical split image of a specimen with black lines showing the borders of the split area.

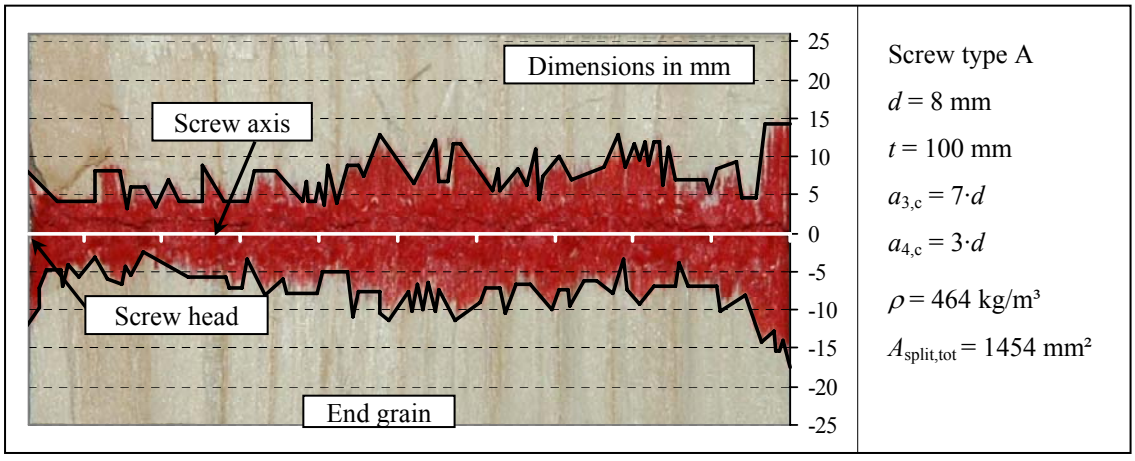

Fig. 13: Opened specimen with red coloured split image, black lines indicating the borders of the split area

4.4 Simulation results and verification

The FE model described in 4.1 is used to calculate the split area for an individual specimen. Therefore it is necessary to adapt the material properties of the volume elements and the spring elements to take into account the specimen's parameters. Additionally the equivalent moving load has to be adjusted. Influences on the equivalent moving load are covered by correction factors:

$$q_{\mathrm{corr}}(x_{\mathrm{Sr}}) = q(x_{\mathrm{Sr}}) \cdot k_{\rho} \cdot k_{\mathrm{r}} \cdot k_{\gamma} \cdot k_{\mathrm{spl}} \tag{2}$$

with

k_{ρ} correction factor for density

k_{r} correction factor for insertion speed

k_{γ} correction factor for the angle between screw-axis and mean growth ring tangent

k_{spl} split area calibration factor

On the basis of test series with the new test method for screw-specific influences - presented in chapter 3 - it was possible to determine the factors k_{ρ} and k_{r}:

$$k_{\rho} = \left(\frac{\rho}{\rho_{\mathrm{ref}}} \right)^2 \tag{3}$$

with

ρ density of the specimen in kg/m³

ρ_{ref} density of the specimen used to determine mean total forces in kg/m³

$$k_{\mathrm{r}} = \left(\frac{U}{U_{\mathrm{ref}}} \right)^{0,063} \tag{4}$$

with

U mean insertion speed in rpm,

U_{ref} insertion speed (rpm) at the tests for mean total forces

An exact calculation of k_{r} is only possible if the rotation speed can be measured e.g. using a screw-testing machine with a known constant and load-independent rotation speed. For customary electric screw drivers the rotation speed under loading is not known and depends on the torsional resistance.

The correction factor for the angle between screw-axis and mean growth ring tangent k_{γ} can be derived by using the special test specimen shown in Fig. 8. As long as k_{γ} is not identified exactly for a screw type by these tests $k_{\gamma} = 1{,}0$ is assumed.

The factor k_{spl} is used to cover further influences and is determined in the process of the model calibration. For the calibration all known parameters and correction factors are calculated and included in the model. By comparing the calculated split areas with the result of calibration test series the factor k_{spl} is derived. Because of the still existent imprecision of the factors k_{r} and k_{γ} the correction factors k_{r}, k_{γ} and k_{spl} were merged to form the factor k_{corr} for the calculations presented here. k_{corr} is determined by using calibration test series as shown in equation (5).

$$k_{\mathrm{corr}} = k_{\mathrm{r}} \cdot k_{\gamma} \cdot k_{\mathrm{spl}} = 1{,}35 \cdot \left(\frac{\rho_{\mathrm{ref}}}{\rho} \right)^{0,8} \tag{5}$$

With equation (5) the equivalent moving load (2) can be calculated as following:

$$q_{\mathrm{corr}}(x_{\mathrm{Sr}}) = q(x_{\mathrm{Sr}}) \cdot k_{\rho} \cdot k_{\mathrm{corr}} \tag{6}$$

Fig. 14 illustrates the resulting split area for one specimen (B.1-01) in comparison to the simulated split area. The results of test and simulation correspond in shape and size.

To verify the calculation model calculated split areas are compared with test results. Fig. 15 shows test results over simulated split areas for three series and three types of screws in each series. The simulated crack areas mostly proved to correspond with the test results.

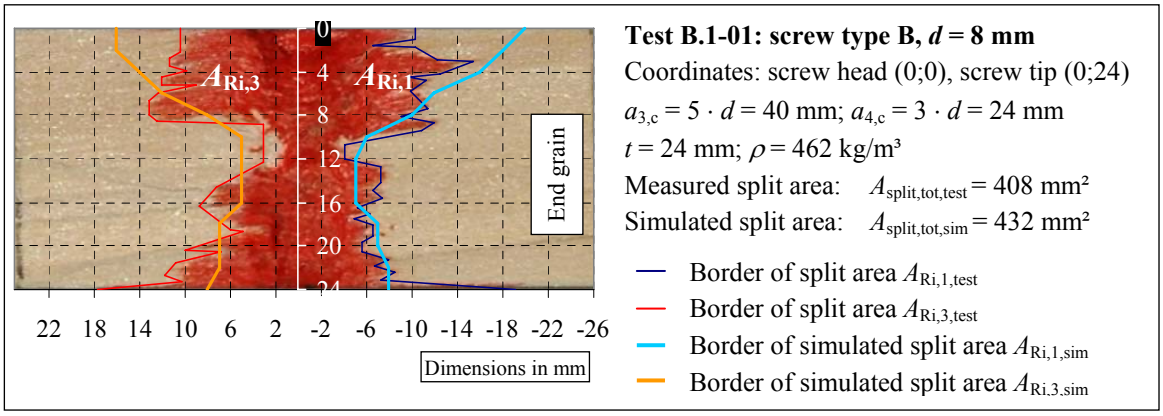

Fig. 14: Split area of test and of calculation for one specimen

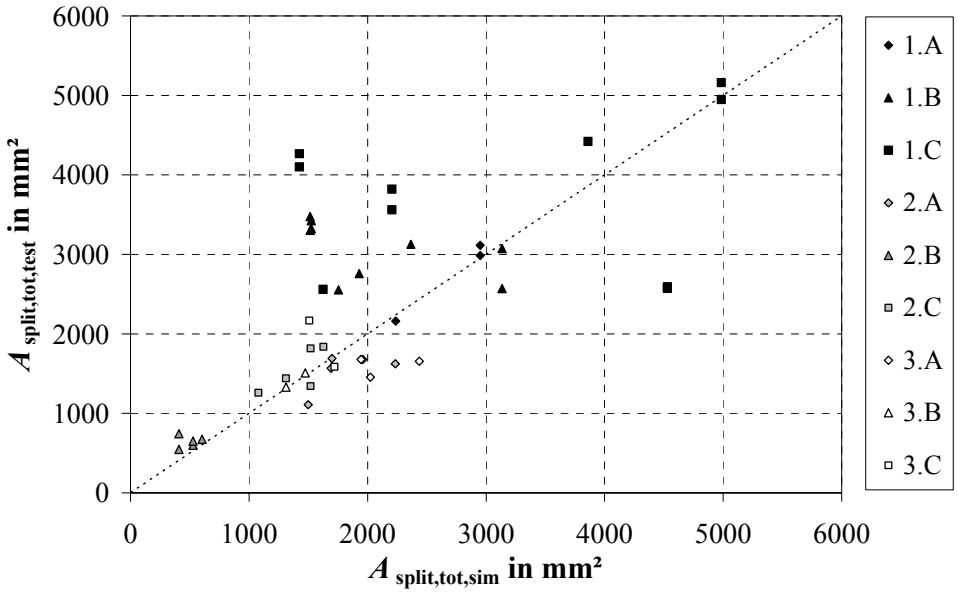

Fig. 15: Measured split areas of tests vs. simulated split areas for nine series

5 Conclusions

To estimate the splitting behaviour of timber during the insertion process a new calculation method was developed. It represents a combination of a FE calculation and a new test method. The FE model allows the calculation of the resulting crack area for screws in different end distances as well as for different cross-sections of timber. In the finite element model the tensile strength perpendicular to the grain that represents a relevant factor for splitting was simulated by using non-linear spring-elements whose material behaviour was determined on the basis of tests using CT specimens.

In order to determine the fastener-specific influences on the splitting behaviour a new test method was developed for measuring forces affecting the member perpendicular to the grain during the insertion process. This method also allows a direct evaluation of a screw's effect on the splitting behaviour by comparing it with the results of parallel tests involving reference screws whose influence on the splitting behaviour has already been established. For the calibration and verification of the model the crack area was visualized in insertion tests by means of dyeing the relevant areas. The simulated crack areas mostly proved to correspond with the test results.

Using the new method reduces the effort of conventional insertion tests and offers a basis for a realistic calculation of the load carrying capacity of joints in the case of failure by splitting.

In the continuation of the research project the parameters influencing the splitting behaviour like e.g. the angle between screw axis and tangent to the annual rings will be determined in greater detail. Besides the influences of the angle between screw axis and grain direction will be examined. In addition, parameters to facilitate the evaluation of the splitting behaviour and their limits (e.g. limits for the dimension of split areas) will be derived.

6 References

[1] DIN 1052:2008-12: Entwurf, Berechnung und Bemessung von Holzbauwerken – Allgemeine Bemessungsregeln und Bemessungsregeln für den Hochbau

[2] EN 1995-1-1:2008-09: Eurocode 5: Design of timber structures – Part 1-1: General – Common rules and rules for buildings.

[3] Blaß H. J., Bejtka I., Uibel T.: Tragfähigkeit von Verbindungen mit selbstbohrenden Holzschrauben mit Vollgewinde. *Karlsruher Berichte zum Ingenieurholzbau*, Band 4, Universitätsverlag Karlsruhe, Germany, 2006

[4] Blaß H. J., Uibel T.: Spaltversagen von Holz in Verbindungen - Ein Rechenmodell für die Rissbildung beim Eindrehen von Holzschrauben. *Karlsruher Berichte zum Ingenieurholzbau*, Band 12, Universitätsverlag Karlsruhe, Germany, 2009, ISBN 978-3-86644-312-915

[5] Lau, P.W.C.; Tardiff, Y.: Progress report: Cracks produced by driving nails into wood – effects of wood and nail variables. Forintek Canada Corp., 1987

[6] Schmid, M.: Anwendung der Bruchmechanik auf Verbindungen mit Holz. Berichte der Versuchsanstalt für Stahl, Holz und Steine, Universität Karlsruhe (TH), Karlsruhe, Germany, 2002.